

EVALUATION OF *IN-VITRO* ANTIMICROBIAL, ANTIOXIDANT AND ANTICANCER ACTIVITY OF A NEW CARBOXYMETHYLCHITOSAN-BASED CYANOQUANIDINE COPOLYMER

NADIA A. MOHAMED^{*,**} and NAHED A. ABD EL-GHANY^{**}

^{*}*Department of Chemistry, College of Science, Qassim University, Buraidah 51452, Saudi Arabia*

^{**}*Department of Chemistry, Faculty of Science, Cairo University, Giza, 12613, Egypt*

✉ *Corresponding authors: N. A. Mohamed, na.ahmed@qu.edu.sa*

N. A. Abd El-Ghany, abdelghanyn@sci.cu.edu.eg

Received February 8, 2024

A new carboxymethylchitosan-based acryloylcyanoguanidine copolymer (CMCS-g-ACG) has been successfully prepared using the grafting technique. The grafting percentage, grafting efficiency, and homopolymer percentage were 86, 85, and 14%, respectively. The chemical structure and surface morphology of the CMCS-g-ACG copolymer were confirmed using elemental analysis, FTIR, ¹H-NMR, XRD, and SEM. The copolymer has greater inhibition activity on both *Escherichia coli* (*E. coli*), *Staphylococcus aureus* (*S. aureus*), and *Candida albicans* (*C. albicans*) in comparison to CMCS. It is more potent against *E. coli* than *S. aureus*. At 2000 µg/mL concentration, CMCS and the copolymer exhibited DPPH scavenging of 63.45% ± 4.19 and 78.56% ± 4.61, respectively. The copolymer of concentration less than 62.5 µg/mL was safe on the normal human lung fibroblast cells. The growth inhibition of the breast cancer cells at 500 µg/mL was 79.59% ± 2.12 and 91.41% ± 2.34 for CMCS and the copolymer, respectively. Thus, the insertion of ACG into CMCS highly boosted its antimicrobial, antioxidant and anticancer characteristics. It is a proper strategy to realize good systems to compete the traditional drugs used for such applications.

Keywords: carboxymethyl chitosan, antimicrobial activity, antioxidant activity, cytotoxicity, breast cancer

INTRODUCTION

Natural biopolymers, particularly chitosan, are gaining popularity in medicine and biotechnology.^{1,2} Chitosan is an amino polysaccharide formed from a random dispersed β-linked D-glucosamine and N-acetyl-D-glucosamine. It has demonstrated exceptional properties, such as biocompatibility, biodegradability, nontoxicity, antimicrobial activity, low immunogenicity, low cost, and ease of use.^{3,4} The insolubility of chitosan in water, due to its rigidity and high crystallinity, leads to a limitation of its use in a wide variety of applications. This drawback can be overcome via preparation of its water-soluble derivatives.^{5,6}

Chemical modification can not only enhance the physico-chemical properties of chitosan, but also keep its wonderful properties and widen the application domains of its modified derivatives. The carboxymethylation reaction at C-6 hydroxyl groups is one of the most appropriate chemical modification processes to improve the solubility

of chitosan in water. The resulting *O*-carboxymethyl chitosan (CMCS) derivative has an amphoteric character, due to the inclusion of both the carboxylic (-COOH) and primary amino (-NH₂) groups in its repeating units. This enables it to be soluble in water at a broad pH range. Thus, it can be used in numerous biomedical applications, such as antimicrobial, drug delivery, wound healing, tissue engineering, and bio-imaging.^{5,7,8} In comparison with chitosan, CMCS showed a greater moisture uptake and a higher water retention,^{9,10} in addition to the improved biological, chelating and adsorption characteristics.¹¹⁻¹³

CMCS has attracted a considerable interest in medicinal and pharmaceutical fields,¹⁴ and exhibited a remarkable anticancer activity.¹⁵ Both chitosan and its diverse derivatives, especially CMCS, can selectively penetrate into the membranes of the cancer cells and exhibit anticancer properties via the antiangiogenic,

cellular enzymatic, antioxidant defense mechanism, immuno-enhancing, and apoptotic pathways.¹⁵ The amphoteric nature of CMCS enhances its ability to form complexes with some heavy metal ions.¹² However, the evolution of some antibiotic-resistant microbial strains has become a serious issue in clinical medicine. For this, the discovery of new chemical compounds, as alternatives to the traditional antibiotics, is on the rise to overcome this problem.¹⁶⁻¹⁸

Chitosan and CMCS show an antioxidant activity due to their possession of active -OH and -NH₂ groups, which can act as free radical scavengers.^{19,20} CMCS exhibits a higher antioxidant potency than virgin chitosan, particularly in terms of its reducing capacity, capability to scavenge DPPH and superoxide radicals, and chelating tendency towards Fe(II) ions.²¹

CMCS hydrogels have shown potential developing prospects in antibacterial,²² antioxidant,²³ and anti-tumor metastasis.²⁴ A CMCS medical scaffold loaded with *Tacrolimus* has shown a promising antibacterial activity for enhancing fibroblast proliferation, angiogenesis and wound dressing.²⁵ Some derivatives of CMCS containing quinoline groups showed excellent antioxidant properties, and an effective capability for scavenging DPPH, hydroxyl radicals, and superoxide anions.²⁶

Guanidine-based derivatives are capable to bind to phosphates, carboxylates, and metals. The guanidinium cations contribute in special interactions between receptors and ligands or substrates and enzymes. Thus, they may have interesting biological activities and pharmaceutical and chemical applications.^{27,28}

Cyanoguanidine is a nitrogen rich organic substance that possesses a guanidine moiety and a cyano group bonded to one of its nitrogen atoms. It has been vastly studied for its pharmaceutical properties, such as antihypertensive and anti-inflammatory activities. Cyanoguanidine also serves as a key intermediate in the synthesis of numerous bioactive materials and has been employed in the development of new herbicides and pesticides.^{29,30}

Guanidinylation of CMCS is considered to be one of the most effective processes to improve its physical and chemical properties, antimicrobial activity, and adsorption capacity of metal ions and dyes for industrial wastewater treatment.³¹⁻³³

Based on the aforementioned antimicrobial and antitumor properties of CMCS, and cyanoguanidine, the present research work was directed to modify CMCS via graft copolymerization using acryloyl cyanoguanidine moieties into its backbone. Elemental analysis, FTIR, ¹H-NMR, XRD, and SEM analyses were used to characterize the chemical and morphological structure of the resulted copolymer. The antimicrobial, antioxidant and anticancer activities of the copolymer were evaluated. The cytotoxicity of the copolymer was also investigated.

EXPERIMENTAL

Materials

Chitosan, with a deacetylation degree of 90% and molecular weight of 2.0×10^5 g/mol, was purchased from Acros Organics (USA). Isopropanol, N,N-dimethyl formamide (DMF) and cyanoguanidine were supplied by Sigma-Aldrich (Germany). Sodium hydroxide pellets were obtained from Loba Chemie (India). Acryloyl chloride, monochloroacetic acid, acetic acid, and potassium persulfate (K₂S₂O₈) were provided by Merck (Germany). Ethanol was obtained from PanReac AppliChem-ITW Reagent (Germany). Methanol was supplied by Chem-Lab (Belgium).

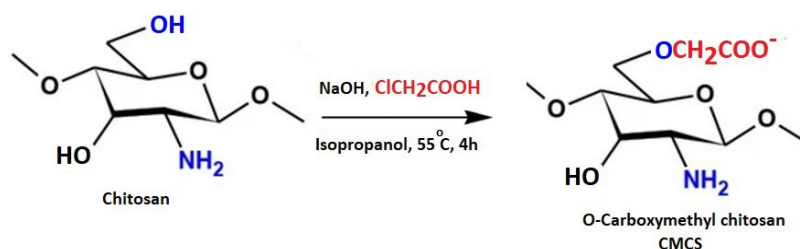
Methods

Synthesis of carboxymethyl chitosan (CMCS)

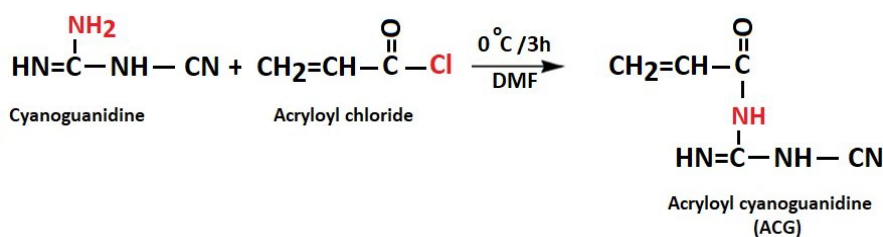
CMCS was prepared based on the procedure reported previously.⁹ Briefly, 10 g of chitosan was stirred in 100 mL of isopropanol containing 13.5 g of sodium hydroxide at room temperature for 1 h to swell and alkalinize. To the resulting suspension, monochloroacetic acid (15 g) was added gradually within 30 min and stirred at 55 °C for 4 h. The reaction mixture was neutralized with 10% (v/v) acetic acid solution, and then isopropanol was discarded. Aqueous ethanol (80%) was added, and the solid product was filtered, rinsed with 80–90% ethanol to desalt and dewater, and vacuum dried at 50 °C. The degree of substitution of CMCS was determined by pH-titration³⁴ and was found to be 0.85 (Scheme 1).

Preparation of acryloyl cyanoguanidine (ACG)

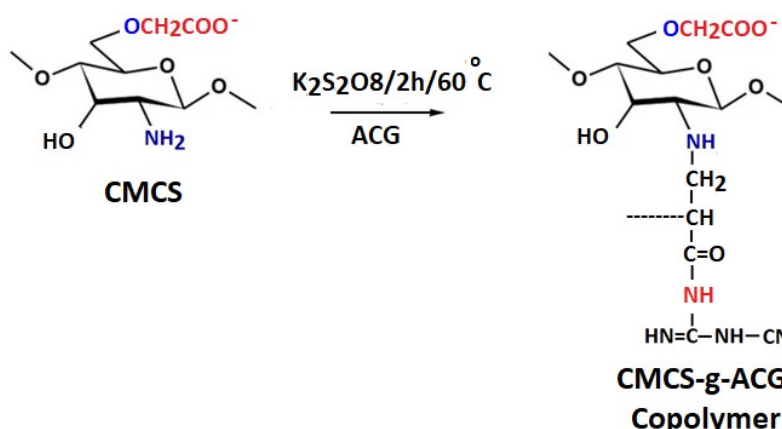
ACG was prepared by dissolving acryloyl chloride (0.1 mol, 9 mL) in 20 mL of DMF and the resulting solution was then cooled in an ice bath. Cyanoguanidine (0.1 mol, 8.4 g) was dissolved in 20 mL of DMF and slowly added to the acryloyl chloride solution. The mixture was kept in an ice bath for 3 h with continuous stirring. After the reaction time was completed, the resulting mixture was poured onto methanol to precipitate the ACG. The latter was washed with methanol and dried in an oven at 60 °C for 8 h (Scheme 2).



Scheme 1: Preparation of CMCS



Scheme 2: Preparation of ACG



Scheme 3: Schematic presentation of preparation of CMCS-g-ACG copolymer

Preparation of CMCS-g-ACG copolymer

Scheme 3 shows the method of preparation of the CMCS-g-ACG copolymer. In a three-necked round-bottom flask, CMCS (0.5 g) was dissolved in double-distilled water (25 mL). To the resulting solution, ACG (1.21 g, 0.35 mol L⁻¹) was slowly added, and the flask was placed in a thermostat bath at 60 °C. Nitrogen gas was bubbled for 30 min under stirring to remove the dissolved oxygen. The graft copolymerization reaction was initiated by a gradual addition of K₂S₂O₈ (0.2 g, 0.03 mol L⁻¹). After 2 h, the resulting copolymer was precipitated in cold methanol, then filtered, washed several times with methanol, and dried under vacuum at 60 °C until a constant weight was obtained. The copolymer was Soxhlet extracted with methanol for 8 h to remove any formed homopolymer. The grafting parameters: grafting percentage (% G), grafting efficiency percentage (% GE) and homopolymer percentage (% H) were determined using Equations (1)–(3):³⁵

$$\% G = [W_2 - W_0 / W_0] \times 100 \quad (1)$$

$$\% GE = [W_1 - W_0 / W_2 - W_0] \times 100 \quad (2)$$

$$\% H = [W_1 - W_2 / W_3] \times 100 \quad (3)$$

where W_0 is the initial CMCS weight, W_1 , and W_2 are the weights of the grafted CMCS before and after Soxhlet extraction, respectively, and W_3 is the weight of the monomer charged. The calculated %G = 86%, %GE = 85% and %H = 14%.

Measurements

Elemental analysis

The changes that arose in the percent of the elements of the formed CMCS, ACG, and CMCS-g-ACG copolymer relative to the virgin chitosan were identified by performing their elemental analysis using a Perkin-Elmer C, H, N, S Analyzer, Model 2410 series II (USA).

Fourier transform infrared (FTIR) spectroscopy

The structure of CMCS, ACG, and CMCS-g-ACG copolymer was investigated using a Tescan Shimadzu FTIR spectrophotometer (Model 8000, Japan). The samples were thoroughly ground with KBr before being compressed under 400 kg/cm² hydraulic pressure

to form pellets, and spectra were recorded in the 400-4000 cm^{-1} range.

¹H-Nuclear magnetic resonance (NMR) spectroscopy

The ¹H-NMR spectrum of the CMCS-g-ACG copolymer was investigated using a JEOL 270 MHz spectrophotometer (Tokyo, Japan) in deuterated dimethyl sulfoxide as a solvent and the chemical shift was recorded in ppm relative to TMS as an internal standard.

X-ray diffraction (XRD) analysis

A Bruker's D-8 advanced wide-angle X-ray diffractometer was used to measure the XRD of the CMCS and CMCS-g-ACG copolymer at room temperature. A nickel filtered CuK radiation (40 kV, 30 mA) produced an X-ray source with a wavelength of 1.5406 Å. The dried samples were mounted on a sample holder and scanned in the reflection mode at an angle 2θ over a range from 4° to 80° at a speed of 8° min^{-1} .

Scanning electron microscopy (SEM) observation

SEM analysis was done using a Hitachi Scanning Electron Microscope (Model S-450) to examine the surface morphology of CMCS and CMCS-g-ACG copolymer. Before examination, the dried samples were loaded onto the surface of an aluminum SEM specimen holder and sputter coated with gold. The accelerating voltage was set at 20 kV.

Antimicrobial assay

The activity of CMCS and CMCS-g-ACG against some microorganisms *S. aureus*, *E. coli*, and *C. albicans* was studied using the Colony Forming Unit Counting Test (CFU). Cultivation and incubation of the suspension of microbes (McFarl and standard 0.5) were done using Mueller-Hinton broth medium for measuring the antimicrobial ratio of the samples. Then, the microbial suspension (200 μL) along with the samples and the DMSO control sample were introduced into a 96-well plate at 37 °C for 24 h. Afterwards, the plates containing dried nutrient agar and covered with microbial solutions (20 μL) were incubated at 37 °C for 24 h. The microbial colonies on the plates were inspected using a digital camera, and their numbers were counted. The antimicrobial performance was expressed using Equation (4):³⁶

$$\text{Antibacterial ratio (\%)} = \frac{(\text{Nr. of CFUs in control group} - \text{Nr. of CFUs in experimental group}) \times 100\%}{\text{Nr. of CFUs in control group}} \quad (4)$$

Antioxidant assay

A freshly prepared methanol solution of 2,2-diphenyl-1-picrylhydrazyl (DPPH) radical (0.004% w/v) was stored at 10 °C in the dark. A methanol solution of the test compound was also prepared. A 40 μL aliquot of the methanol solution was added to 3 mL

of DPPH solution. Absorbance measurements were recorded immediately with a UV-visible spectrophotometer (Milton Roy, Spectronic 1201). The decrease in absorbance at 515 nm was determined continuously, with data being recorded at 1 min intervals until the absorbance stabilized (16 min). The absorbance of the DPPH radical without antioxidant (control) and the reference compound – ascorbic acid – was also measured. All the determinations were performed in three replicates and averaged. The percentage inhibition (PI) of the DPPH radical was calculated according to Equation (5):³⁷

$$\text{PI} = \left[\frac{(AC - AT)}{AC} \right] \times 100 \quad (5)$$

where AC = absorbance of the control at t = 0 min and AT = absorbance of the sample + DPPH at t = 16 min.

The 50% inhibitory concentration (IC_{50}), the concentration required to inhibit DPPH radical by 50%, was estimated from graphic plots of the dose response curve.

Cytotoxicity assay

The toxic effect of the CMC-g-ACG copolymer on normal human lung fibroblast cells (WI-38 cell line) was inspected using the viability assay that was previously described.³⁸ An Olympus inverted microscope, model CKX41 (Japan), provided with a digital microscopy camera, was employed to inspect the changes in the cellular morphology of the treated cells in comparison with the non-treated cells. The cytopathic effects and, consequently, the morphological alterations were visualized at a magnification of 100x.

Anticancer assay

For the anticancer assay, the MCF-7 cells (human breast cancer cell line) were suspended in medium at the concentration of 5×10^4 cell/well in Corning® 96-well tissue culture plates, then incubated for 24 h. The tested compounds were then added into 96-well plates (three replicates) to achieve twelve concentrations for each compound. Six vehicle controls with media or 0.5% DMSO were run for each 96 well plate as a control. After incubating for 48 h, the numbers of viable cells were determined by the MTT test. Briefly, the media were removed from the 96 well plate and replaced with 100 μL of fresh culture RPMI 1640 medium, without phenol red, then 10 μL of the 12 mM MTT stock solution (5 mg of MTT in 1 mL of PBS) was added to each well, including the untreated controls. The 96 well plates were then incubated at 37 °C and 5% CO_2 for 4 h. An aliquot of the media (85 μL) was removed from the wells, and 50 μL of DMSO was added to each well, mixed thoroughly with the pipette and incubated at 37 °C for 10 min. Then, the optical density was measured at 590 nm with the microplate reader (SunRise, TECAN, Inc, USA) to determine the number of viable cells and the percentage of viability was calculated using Equation (6):

$$[(OD_t/OD_c)] \times 100\% \quad (6)$$

where OD_t is the mean optical density of wells treated with the tested sample and OD_c is the mean optical density of non-treated cells.

The relation between surviving cells and drug concentration was plotted to get the survival curve of each tumor cell line after treatment with the specified compound. The 50% inhibitory concentration (IC_{50}), the concentration required to cause toxic effects in 50% of intact cells, was estimated from graphic plots of the dose response curve for each concentration using GraphPad Prism software (San Diego, CA, USA).^{38,39}

RESULTS AND DISCUSSION

FTIR spectroscopy of CMCS and CMCS-g-ACG copolymer

Figure 1 shows the FTIR spectra of ACG, CMCS and CMCS-g-ACG copolymer. The spectrum of ACG displays characteristic peaks at 3334 cm^{-1} corresponding to NH_2 , at 3165 cm^{-1} related to $=\text{C}-\text{H}$, and at 2194 and 2155 cm^{-1} attributed to the CN stretching vibration.⁴⁰ The peaks at 1698 and 1637 cm^{-1} are related to the $\text{C}=\text{O}$ and $\text{C}=\text{C}$ groups, respectively, while the peaks at 1515 and 1456 cm^{-1} are assigned to the NH bending vibration and $\text{C}=\text{N}$ stretching vibration, respectively, and that at 1372 cm^{-1} is ascribed to the bending CH groups. The peak at 1276 cm^{-1} is attributed to the $\text{C}-\text{N}$ groups.⁴¹

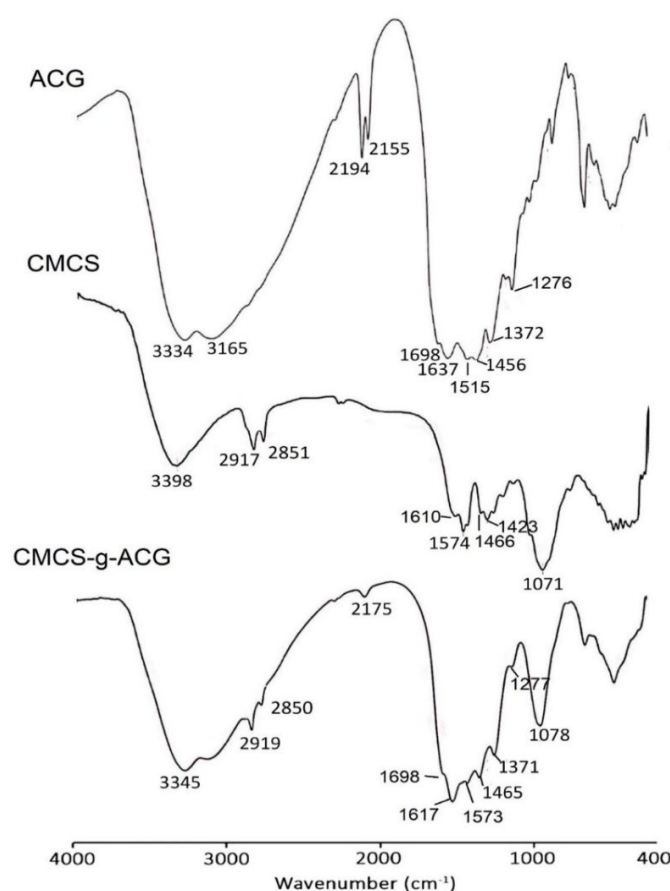


Figure 1: FTIR spectra of ACG, CMCS and CMCS-g-ACG copolymer

The FTIR spectrum of CMCS shows characteristic peaks at 3398 cm^{-1} corresponding to the overlapped stretching vibration of OH and NH_2 groups, and at 2917 and 2851 cm^{-1} related to the stretching vibration of CH , CH_2 groups. The peaks at 1610 and 1574 cm^{-1} are assigned to the asymmetric and symmetric vibrations of the COOH groups, respectively. The peaks at 1466

and 1423 cm^{-1} are attributed to the bending NH and CH groups, respectively, and the peak at 1071 cm^{-1} corresponds to the $\text{C}-\text{OH}$ groups.⁴² The FTIR spectrum of CMCS-g-ACG copolymer shows almost all of the above-mentioned peaks, but with the absence of the peaks related to the $\text{C}=\text{C}$ groups at 1637 and 1637 cm^{-1} , which confirms the grafting process.

¹H-NMR spectroscopy of CMCS and CMCS-g-ACG copolymer

Figure 2 shows the ¹H-NMR spectra of ACG, CMCS and their CMCS-g-ACG copolymer (solvent, deuterated DMSO). In the ACG spectrum, the signal that appeared at $\delta = 2.808$ ppm represented the overlapped CH₂ and CH protons, while that for the NH protons appeared as a broad one from $\delta = 6.118$ to 6.845 ppm. The spectrum of CMCS shows characteristic signals at $\delta = 1.995$ ppm, attributed to the protons on carbons 2, 3 and 4, and at 2.774 ppm, related to the protons on carbons 1, 5 and 6. The signals of the protons on carbon 7 and the OH proton appearing at $\delta = 3.995$ and 4.022 ppm, respectively, the signal at $\delta = 8.59$ ppm corresponding to the NH₂ protons, while the signal at 10.01 ppm is assigned to the COOH proton.

Moreover, the spectrum of CMCS-g-ACG copolymer combined the signals of both CMCS and ACG. It exhibited a strong signal in the region ranging from $\delta = 1.024$ to 1.045 ppm, which represents the protons on carbons 2, 3, 4 and 8, while the signal at 1.231 ppm is related to the proton on carbon 5, and the signal at 1.888 ppm can be attributed to the protons on carbons 1 and 6. The strong signal at 2.499 ppm is assigned to the protons on carbons 7, 9 and OH proton. On the other hand, there are a number of signals in the region ranging from $\delta = 6.012$ to 8.029 ppm, corresponding to the NH groups. Meanwhile, the signal at $\delta = 9.987$ ppm can be ascribed to the proton of -COOH group. These spectral data confirm the formation of the CMCS-g-ACG copolymer.

XRD analysis of CMCS and CMCS-g-ACG copolymer

XRD was used to investigate the morphology of CMCS and CMCS-g-ACG copolymer, as shown in Figure 3. The pattern suggested that the introduction of graft molecules onto the CMCS chains had a significant impact on its morphological structure. The graft molecules break the intermolecular hydrogen bonds between the -COOH, -NH₂ and -OH groups of the neighboring chains and separate them from each other. This results in a significantly decreased crystallinity of the matrix and the formation of a highly amorphous copolymer structure. This result agrees well with the XRD patterns of CMCS grafted with terephthaloyl thiourea

linkages,²² pyromellitimide benzoyl thiourea moieties,³⁴ and N-acryloyl,N'-cyanoacetohydrazide monomer.⁴¹

SEM analysis of CMCS and CMCS-g-ACG copolymer

The changes that occurred on the surface of CMCS after the grafting process were observed using scanning electron microscopy. The images showed that, compared to CMCS, the surface structure of the CMCS-g-ACG copolymer appeared to be full of lumps as a result of the grafting process and to have many pores as a result of the ionic interaction between the -COO⁻ groups of the CMCS and the -NH groups of the guanidine moiety, as shown in Figure 4. An additional proof for the grafting of CMCS with ACG comes from the elemental analysis of ACG, CMCS and CMCS-g-ACG copolymer, as shown in Table 1. There are appreciable changes in the percentage of the elements, particularly nitrogen, between them, confirming that the graft copolymerization process was successfully accomplished. As compared with the virgin CMCS, the results disclosed that CMCS-g-ACG copolymer displayed a considerable increase in nitrogen percent on the expense of other elements, due to insertion of ACG moieties into its repeating units.

***In vitro* antimicrobial activity of CMCS and CMCS-g-ACG copolymer**

The antimicrobial activity of CMCS and CMCS-g-ACG copolymer was investigated against Gram-positive bacteria (*S. aureus*), Gram-negative bacteria (*E. coli*), and fungi (*C. albicans*) using the Colony Forming Unit Counting Test (CFU). The obtained data illustrated that both CMCS and CMCS-g-ACG copolymer exhibited appreciable activity in inhibiting the proliferation of the tested strains (Fig. 5). It was found that the CMCS-g-ACG copolymer was more potent in inhibiting the microbial/fungal activity than CMCS, since it displayed an inhibition of 30% \pm 2.5, 33.3% \pm 3.3, and 36.8% \pm 4.9 against *S. aureus*, *E. coli* and *C. albicans*, respectively, compared to 14% \pm 3.1, 13% \pm 1.6, and 21.1% \pm 3.9 of the CMCS based on the number of inhibited colonies. Thus, the inhibition performance of the copolymer exceeds by more than 2.5 times, more than 2 times, and more than 1.7 times that achieved when CMCS was used for *E. coli*, *S. aureus*, and *C. albicans*, respectively.

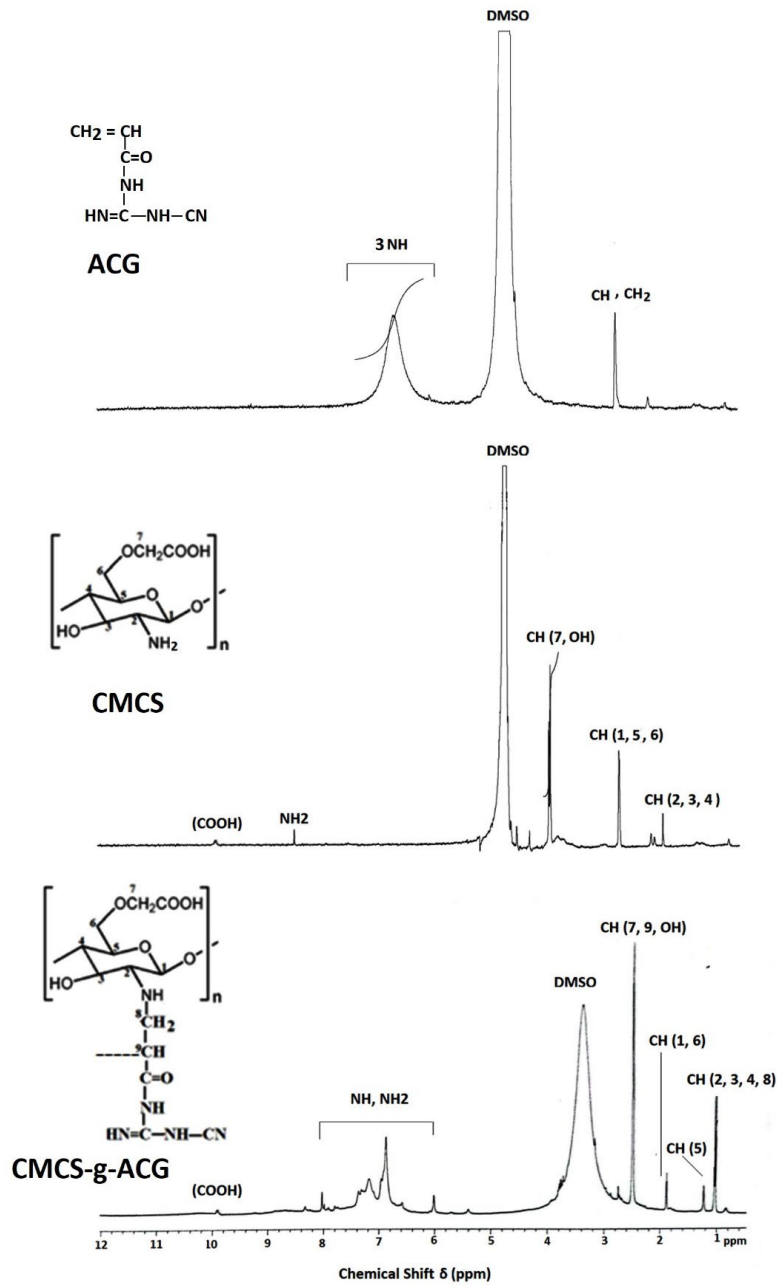


Figure 2: ¹H-NMR spectra of ACG, CMCS and CMCS-g-ACG copolymer

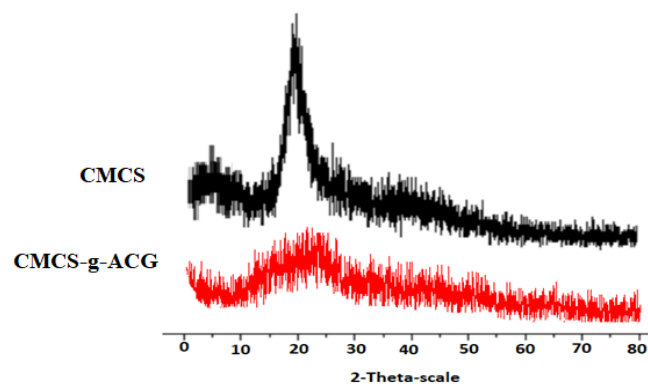


Figure 3: XRD patterns of CMCS and CMCS-g-ACG copolymer

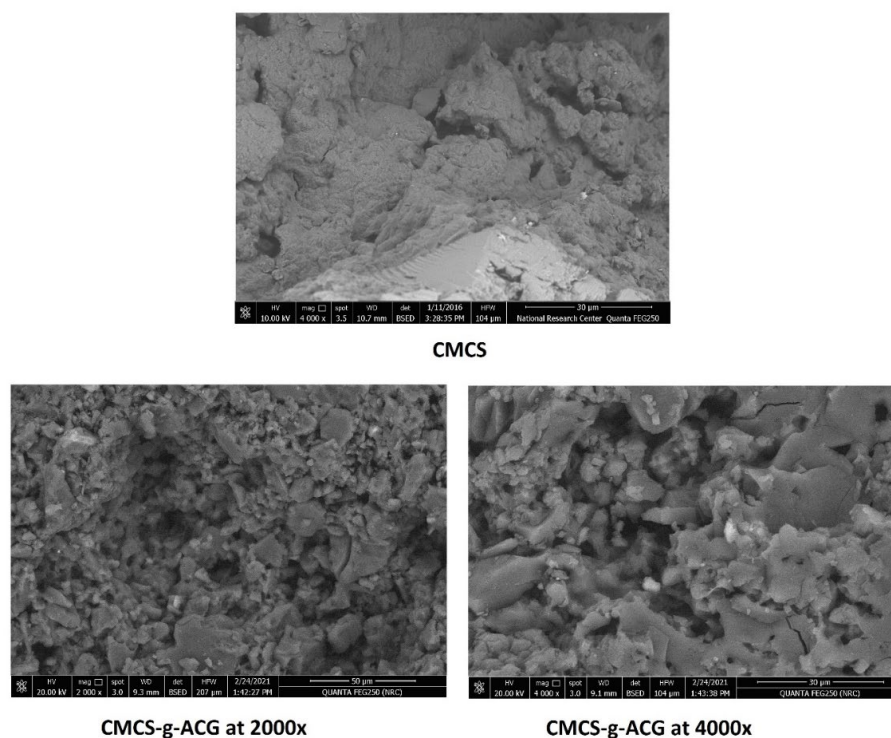


Figure 4: SEM images of CMCS and CMCS-g-ACG copolymer

Table 1
Elemental analysis of CMCS, ACG, and CMCS-g-ACG copolymer

Sample	Elemental analysis (%)			
	C	H	N	O
CMCS	44.20	6.01	6.53	43.26
ACG	43.48	4.34	40.58	11.60
CMCS-g-ACG	44.06	5.24	17.80	32.90

The better inhibition performance of the copolymer may be attributed to the increase in its cationic sites due to the nitrogen-rich ACG moieties incorporated in its matrices, since their NH, C=O, and CN groups could be protonated. This enhanced the copolymer interaction with the anionic microbial cell membranes via electrostatic forces, resulting in a change in their permeability, causing imbalances in the internal osmotic pressure, and thus inhibiting the growth of the microbes. Also, this interaction may lead to hydrolysis of the peptidoglycans in the microbial cell membranes, leading to a leak of the internal cellular electrolytes, such as potassium ions, and other low molecular weight proteinaceous components, such as protein, nucleic acid, glucose, and lactate dehydrogenase.⁴³ Further, the

higher antimicrobial activity of the copolymer might be due to its greater hydrophilic properties, which allow it to penetrate inside the microbial cells, disturbing their function; it binds with the cell DNA, preventing the formation of RNA and proteins, and thus inhibiting the microbial growth.⁴³ Moreover, the greater antimicrobial behavior of the copolymer resulted from the grafted cyanoguanidine moieties, which act as potent chelating centers for suppression of spore elements and binding to essential nutrients for microbial growth.^{44,45} This explains the better antibacterial effect of the copolymer, compared to the virgin CMCS. Analogous findings were reported for the antimicrobial activity of chitosan, CMCS, and their hydrogels.^{22,25}

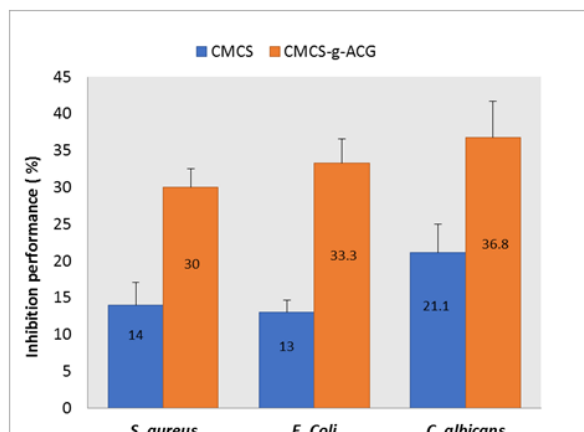


Figure 5: Antimicrobial behavior of CMCS and CMCS-g-ACG copolymer against *S. aureus*, *E. coli* and *C. albicans*

***In vitro* antioxidant activity of CMCS and CMCS-g-ACG copolymer**

Free radicals are formed in biological systems as a result of metabolic processes and the oxidative degradation of nutrients.⁴⁶ The majority of free radicals, produced by molecular oxygen (O_2) during energy production in mitochondria, are referred to as reactive oxygen species (ROS). The most common ROS are superoxide (O_2^-), hydrogen peroxide (H_2O_2), and hydroxyl radicals. In a healthy organism, oxidants (free radicals) and antioxidant levels are normally balanced.⁴⁷ If the balance between free radicals and antioxidants is disrupted, free radicals or ROS begin to cause damage (oxidative stress) to cell components. Free radicals are commonly associated with aging and diseases, such as diabetes, cancer, inflammation, neurological disorders, and diuretics.⁴⁸ As a result, elimination of excess ROS from the body can effectively postpone cellular senescence, inhibit malignant tumors, and prevent inflammation.²⁶ The antioxidant activities of chitosan and CMCS suggest that the active hydroxyl and amino groups within polymer chains may participate in free radical scavenging. CMCS has been proven a better antioxidant than native chitosan, particularly in terms of reducing power and DPPH scavenging ability.^{21,49} CMCS is used as an antioxidant in the pharmaceutical, biomedical, and environmental fields, because it acts as an electron donor to convert free radicals into more stable products, thereby terminating free radical chain reactions.⁵⁰ The large number of intramolecular and intermolecular hydrogen bonds formed between the COOH groups in CMCS reduces the interaction of the amino groups with the free radical. Cyanoguanidine

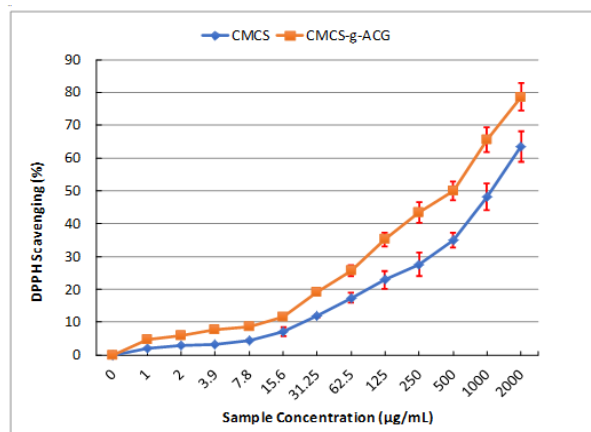


Figure 6: DPPH radical scavenging activity of CMCS and CMCS-g-ACG copolymer

derivatives possess a variety of biological activities, including antioxidant, antihypertensive, anticancer, antihistaminic, and antimicrobial properties.⁴⁸ Incorporation of the cyanoguanidine moieties into CMCS, separate its chains from each another, enhancing free radical scavenging by the NH, OH, C=NH and C \equiv N groups in CMCS-g-ACG copolymer.

The DPPH assay is the most commonly used method for determining free radical scavenging activity. It has been proposed that after accepting hydrogen radicals or an electron, DPPH becomes a stable molecule.⁵¹ The free radical scavenging activity of CMCS-g-ACG copolymer was determined using ascorbic acid as a reference drug. Figure 6 shows the percentages of free radical scavenging activity for various copolymer concentrations. In comparison with CMCS, CMCS-g-ACG copolymer exhibited a higher free radical scavenging activity at all the used concentrations. The concentration that results in scavenging of 50% of free radicals (IC_{50}) was $1116.29 \pm 4.73 \mu\text{g/mL}$ and $500 \pm 2.34 \mu\text{g/mL}$ for CMCS and the copolymer, respectively. At a higher concentration, of $2000 \mu\text{g/mL}$, CMCS and the copolymer exhibited free radical scavenging of $63.45\% \pm 4.19$ and $78.56\% \pm 4.61$, respectively. Similar results were illustrated in some previous studies for the free radical scavenging activity of chitosan, CMCS, and CMCS-based quinoline derivatives.^{19-21,23,26}

***In vitro* cytotoxic effect of CMCS-g-ACG copolymer**

The toxic effect of CMCS-g-ACG copolymer of different concentrations, ranging from 0 to $500 \mu\text{g/mL}$, was investigated on normal human lung

fibroblast cells (WI-38 cell line), according to the previously reported viability assay,³⁸ and the results were shown in Figure 7. The results indicated that the copolymer of concentrations less than 62.5 µg/mL did not have any impact on the examined cells viability, while at 62.5 µg/mL, it showed a slight inhibitory action of 1.86% ± 0.62. Thus, it is not recommended to use the copolymer in a dose higher than 62.5 µg/mL. The cells viability decreased with an increase in the copolymer concentration. The copolymer displayed a perceivable cytotoxic action on the inspected cells at its high concentrations, since the cells viability at 125, 250, and 500 µg/mL

copolymer concentrations were 86.27% ± 1.47, 62.91% ± 2.85, and 28.75% ± 3.19, respectively. Further, the cytotoxic concentration (IC₅₀) that led to toxicity in 50% of intact cells was 344 ± 1.23 µg/mL. The cytotoxic effect of CMCS-g-ACG copolymer might be due to the presence of the -COOH and CN groups, which can attack the cell functional protein, cause its aggregation and prevent the formation of DNA. This can lead to the death of the cells.²⁷ Moreover, Figure 8 illustrates the microscopic screening of the inspected cells that were incubated in the presence of the copolymer at concentrations of 125, 250 and 500 µg/mL for 24 h.

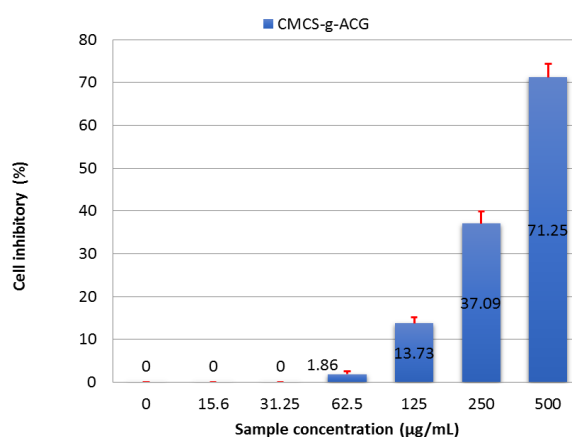


Figure 7: Cytotoxicity activity of CMCS-g-ACG copolymer against normal human lung fibroblast cells (WI-38 cell line)

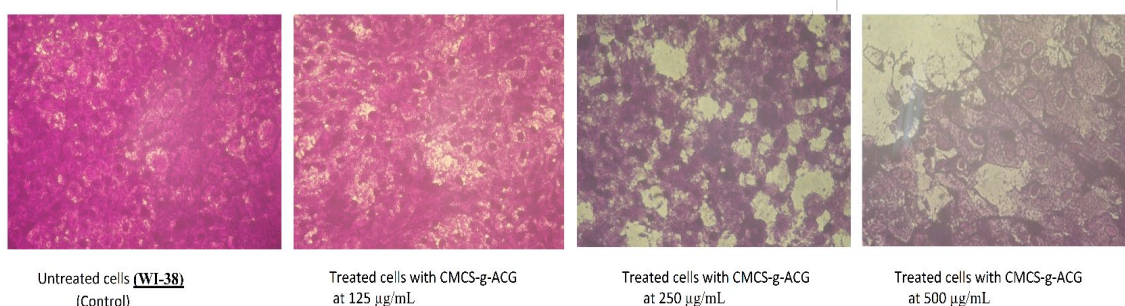


Figure 8: Microscopic examination of normal human lung fibroblast cells (WI-38 cell line) incubated with CMCS-g-ACG copolymer of 125, 250 and 500 µg/mL concentrations for 24 h compared with untreated cells (control cells)

***In vitro* anticancer effect of CMCS and CMCS-g-ACG copolymer**

The *in vitro* anticancer activity of CMCS and CMCS-g-ACG copolymer of different concentrations ranging from 0 to 500 µg/mL was investigated against human breast cancer cells (MCF-7 cell line) using the MTT assay, and the results are shown in Figure 9. Both CMCS and the copolymer have significant anticancer activity, especially at higher concentrations. The results showed that the copolymer was more

effective in inhibiting the growth of human breast cancer cells, whereas the percent of cell inhibition at 500 µg/mL was 79.59% ± 2.12 and 91.41% ± 2.34 for CMCS and the copolymer, respectively. The concentrations of CMCS and the copolymer that inhibited the growth of 50% of the human breast cancer cells (IC₅₀) were 60.5 ± 2.11 µg/mL and 30.5 ± 2.39 µg/mL, respectively. The higher anticancer activity of the CMCS and CMCS-g-ACG copolymer resulted from their hydrophilic character, which allowed easy penetration inside

the cells, causing disturbances in normal functioning of the cells' cycle, interfering with the biological system from DNA to RNA to protein or enzymatic synthesis, and the disruption of the hormonal path to inhibit the growth of cancer cells. It is worth mentioning that both chitosan and its various derivatives have been reported to selectively permeate through the cancer cell membranes and show anticancer activity through the cellular enzymatic, antiangiogenic, immuno-enhancing, antioxidant defense mechanism, and apoptotic pathways.¹⁵ As published previously, cyanoguanidine derivatives were found to exert potent cytotoxic effects in human breast and lung cancer cell lines, with lesser effects on normal fibroblasts and endothelial cells.⁵² Accordingly, the CMCS-g-ACG copolymer exhibited a greater

potential anticancer effect than CMCS alone. It is interesting to mention that, from the cytotoxicity examination (Fig. 7), the copolymer had no effect on the intact cells at concentrations below 62.5 $\mu\text{g}/\text{mL}$. Thus, the copolymer can be used as a breast cancer inhibitor without hazardous effects on intact cells when used at low concentrations. Also, Figure 10 shows the microscopic screening of the breast cancer cells (MCF-7 cell line) that were incubated in the presence of the copolymer at concentrations of 125, 250 and 500 $\mu\text{g}/\text{mL}$ for 24 h, in comparison with the untreated cells (control cells). These findings are in agreement with some previous studies regarding the anticancer activity of chitosan, CMCS, and their various derivatives.^{15,24}

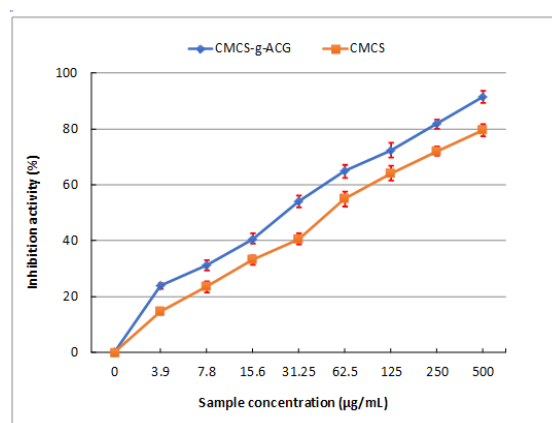


Figure 9: Anticancer activity of CMCS and CMCS-g-ACG copolymer against human breast cancer cells (MCF-7 cell line)

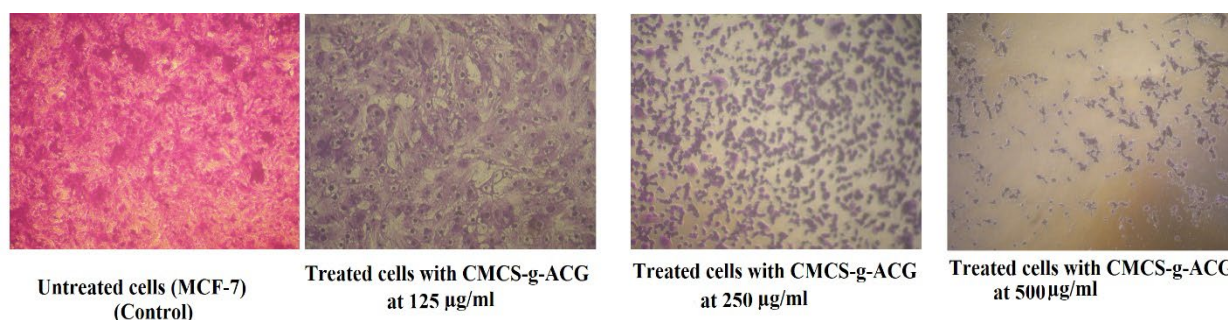


Figure 10: Microscopic examination of human breast cancer cells (MCF-7 cell line) incubated with CMCS-g-ACG copolymer of 125, 250 and 500 $\mu\text{g}/\text{mL}$ concentrations for 24 h, compared with untreated cells (control cells)

CONCLUSION

A new graft copolymer was prepared via copolymerization of ACG onto CMCS. The chemical structure of the produced CMCS-g-ACG copolymer was proved using elemental analysis, and FTIR and $^1\text{H-NMR}$ spectroscopy. Its surface and inner morphology were inspected by

SEM and XRD techniques, respectively. The copolymer showed an amorphous structure relative to CMCS. Its antimicrobial performance can be ranked as follows: *C. albicans* > *E. coli* > *S. aureus*. The copolymer possesses a greater free radical scavenging activity than CMCS, since the concentrations that lead to scavenging of 50% of

free radicals (IC₅₀) were 500 ± 2.34 µg/mL and 1116.29 ± 4.73 µg/mL for the copolymer and CMCS, respectively. The copolymer was safe when used at concentrations less than 62.5 µg/mL on normal human lung fibroblast cells (WI-38 cell line). The copolymer has a greater potency in inhibiting the growth of human breast cancer cells (MCF-7 cell line), whereas the percent of cell inhibition at 31.25 µg/mL was 53.87% ± 2.41 and 40.5% ± 1.98 for the copolymer and CMCS, respectively. Accordingly, it can be concluded that this copolymer can be used as an effective antimicrobial, antioxidant and anticancer agent to be applied in the biomedical and pharmacological domains.

REFERENCES

- 1 N. Desai, D. Rana, S. Salave, R. Gupta, P. Patel *et al.*, *Pharmaceutics*, **15**, 1313 (2023), <https://doi.org/10.3390/pharmaceutics15041313>
- 2 N. Y. Elmehbad, N. A. Mohamed, N. A. Abd El-Ghany and M. M. Abdel-Aziz, *Int. J. Biol. Macromol.*, **253**, 127277 (2023), <https://doi.org/10.1016/j.ijbiomac.2023.127277>
- 3 I. Aranaz, A. R. Alcántara, M. C. Civera, C. Arias, B. Elorza *et al.*, *Polymers*, **13**, 3256 (2021), <https://doi.org/10.3390/polym13193256>
- 4 R. A. Alharbi, F. M. Alminderej, N. F. Al-Harby, N. Y. Elmehbad and N. A. Mohamed, *Polymers*, **15**, 980 (2023), <https://doi.org/10.3390/polym15040980>
- 5 Y. Geng, H. Xue, Z. Zhang, A. C. Panayi, S. Knoedler *et al.*, *Carbohydr. Polym.*, **305**, 120555 (2023), <https://doi.org/10.1016/j.carbpol.2023.120555>
- 6 N. A. Mohamed, M. W. Sabaa, A. H. El-Ghandour, M. M. Abdel-Aziz and O. F. Abdel-Gawad, *Int. J. Biol. Macromol.*, **60**, 156 (2013), <https://doi.org/10.1016/j.ijbiomac.2013.05.022>
- 7 Z. Shariatinia, *Int. J. Biol. Macromol.*, **120**, 1406 (2018), <https://doi.org/10.1016/j.ijbiomac.2018.09.131>
- 8 N. A. Mohamed and N. A. Abd El-Ghany, *Int. J. Biol. Macromol.*, **50**, 1280 (2012), <https://doi.org/10.1016/j.ijbiomac.2012.03.011>
- 9 N. A. Abd El-Ghany, *J. Carbohydr. Chem.*, **36**, 31 (2017), <https://doi.org/10.1080/07328303.2017.1353610>
- 10 N. A. Mohamed and N. A. Abd El-Ghany, *Cellulose Chem. Technol.*, **50**, 463 (2016), [https://www.cellulosechemtechnol.ro/pdf/CCT3-4\(2016\)/p.463-471.pdf](https://www.cellulosechemtechnol.ro/pdf/CCT3-4(2016)/p.463-471.pdf)
- 11 R. C. Gonçalves, R. Signini, L. M. Rosa, Y. S. P. Dias, M. C. Vinaud *et al.*, *Acta Cir. Bras.*, **36**, e360303 (2021), <https://doi.org/10.1590/ACB360303>
- 12 Z. Liu, X. Mo, F. Ma, S. Li, G. Wu *et al.*, *Carbohydr. Polym.*, **261**, 117869 (2021), <https://doi.org/10.1016/j.carbpol.2021.117869>
- 13 N. F. Al-Harby, R. S. Almutairi, N. Y. Elmehbad and N. A. Mohamed, *Polym. Eng. Sci.*, **63**, 2336 (2023), <https://doi.org/10.1002/pen.26380>
- 14 B. Fonseca-Santos and M. Chorilli, *Mater. Sci. Eng. C Mater. Biol. Appl.*, **77**, 1349 (2017), <https://doi.org/10.1016/j.msec.2017.03.198>
- 15 H. S. Adhikari and P. N. Yadav, *Int. J. Biomater.*, **2018**, 2952085 (2018), <https://doi.org/10.1155/2018/2952085>
- 16 N. Y. Elmehbad, N. A. Mohamed, N. A. Abd El-Ghany and M. M. Abdel-Aziz, *Int. J. Biol. Macromol.*, **246**, 125582 (2023), <https://doi.org/10.1016/j.ijbiomac.2023.125582>
- 17 R. T. Alfuraydi, F. M. Alminderej and N. A. Mohamed, *Polymers*, **14**, 1619 (2022), <https://doi.org/10.3390/polym14081619>
- 18 N. A. Mohamed and N. A. Abd El-Ghany, *Cellulose*, **26**, 1141 (2019), <https://doi.org/10.1007/s10570-018-2096-5>
- 19 G. Q. Ying, W. Y. Xiong, H. Wang, Y. Sun and H. Z. Liu, *Carbohydr. Polym.*, **83**, 1787 (2011), <https://doi.org/10.1016/j.carbpol.2010.10.037>
- 20 A. Zimoch-Korzycka, Ł. Bobak and A. Jarmoluk, *Int. J. Mol. Sci.*, **17**, 1436 (2016), <https://doi.org/10.3390/ijms17091436>
- 21 D. Zhao, J. Huang, S. Hu, J. Mao and L. Mei, *Carbohydr. Polym.*, **85**, 832 (2011), <https://doi.org/10.1016/j.carbpol.2011.04.007>
- 22 N. A. Mohamed and N. A. Abd El-Ghany, *Cellulose*, **19**, 1879 (2012), <https://doi.org/10.1007/s10570-012-9789-y>
- 23 Q. Wei, Y. Wang, H. Wang, L. Qiao, Y. Jiang *et al.*, *Carbohydr. Polym.*, **278**, 119000 (2022), <https://doi.org/10.1016/j.carbpol.2021.119000>
- 24 Z. Jiang, B. Han, H. Li, X. Li, Y. Yang *et al.*, *Carbohydr. Polym.*, **125**, 53 (2015), <https://doi.org/10.1016/j.carbpol.2015.02.039>
- 25 S. Al-Hashmi, S. Vakilian, F. Jamshidi-Adegani, J. Al-Kindi, F. Al-Fahdi *et al.*, *J. Drug Deliv. Sci. Technol.*, **86**, 104707 (2023)
- 26 L. Wang, R. Guo, X. Liang, Y. Ji, J. Zhang *et al.*, *Mar. Drugs*, **21**, 606 (2023), <https://doi.org/10.3390/md21120606>
- 27 F. Estévez-Sarmiento, E. Saavedra, I. Brouard, J. Peyrac, J. Hernández-Garcés *et al.*, *Int. J. Mol. Sci.*, **23**, 15518 (2022), <https://doi.org/10.3390/ijms232415518>
- 28 N. A. Mohamed, *Polym. Degrad. Stab.*, **44**, 33 (1994), [https://doi.org/10.1016/0141-3910\(94\)90029-9](https://doi.org/10.1016/0141-3910(94)90029-9)
- 29 S. A. A. Abdel-Raheem, A. M. Drar, B. R. M. Hussein and A. H. Moustafa, *Curr. Chem. Lett.*, **12**, 695 (2023), <https://doi.org/10.5267/j.ccl.2023.5.005>
- 30 R. F. Al-Ghamdi, M. M. Fahmi and N. A. Mohamed, *Polym. Degrad. Stab.*, **91**, 1530 (2006), <https://doi.org/10.1016/j.polymdegradstab.2005.10.001>
- 31 N. A. Mohamed, *Polymer*, **38**, 4705 (1997), [https://doi.org/10.1016/S0032-3861\(96\)01081-6](https://doi.org/10.1016/S0032-3861(96)01081-6)

- ³² Y. Ding, J. Yang and J. Cai, *Int. J. Environ. Anal. Chem.*, **98**, 1275 (2018), <https://doi.org/10.1080/03067319.2018.1545901>
- ³³ N. F. Al-Harby, E. F. Albahly and N. A. Mohamed, *Polymers*, **13**, 4446 (2021), <https://doi.org/10.3390/polym13244446>
- ³⁴ N. A. Mohamed and N. A. Abd El-Ghany, *Int. J. Polym. Mater. Polym. Biomater.*, **66**, 861 (2017), <https://doi.org/10.1080/00914037.2017.1280794>
- ³⁵ N. A. Abd El-Ghany, M. S. Abdel Aziz, M. M. Abdel-Aziz and Z. Mahmoud, *Int. J. Biol. Macromol.*, **134**, 912 (2019), <https://doi.org/10.1016/j.ijbiomac.2019.05.078>
- ³⁶ Y. Xiang, X. Liu, C. Mao, X. Liu, Z. Cui *et al.*, *Mater. Sci. Eng. C*, **85**, 214 (2018), <https://doi.org/10.1016/j.msec.2017.12.034>
- ³⁷ G. C. Yen and P. D. Duh, *J. Agric. Food Chem.*, **42**, 629 (1994), <https://doi.org/10.1021/jf00039a005>
- ³⁸ T. Mosmann, *J. Immunol. Methods*, **65**, 55 (1983), [https://doi.org/10.1016/0022-1759\(83\)90303-4](https://doi.org/10.1016/0022-1759(83)90303-4)
- ³⁹ N. Y. Elmehbad, N. A. Mohamed and N. A. Abd El-Ghany, *Int. J. Biol. Macromol.*, **205**, 719 (2022), <https://doi.org/10.1016/j.ijbiomac.2022.03.076>
- ⁴⁰ N. A. Mohamed and M. W. Sabaa, *Polym. Int.*, **45**, 147 (1998), [https://doi.org/10.1002/\(SICI\)1097-0126\(199802\)45:2<147::AID-PI851>3.0.CO;2-%23](https://doi.org/10.1002/(SICI)1097-0126(199802)45:2<147::AID-PI851>3.0.CO;2-%23)
- ⁴¹ N. A. Mohamed and N. A. Abd El-Ghany, *J. Carbohydr. Chem.*, **31**, 220 (2012), <https://doi.org/10.1080/07328303.2011.650338>
- ⁴² N. F. Al-Harby, R. S. Almutairi and N. A. Mohamed, *Polymers*, **13**, 3659 (2021), <https://doi.org/10.3390/polym13213659>
- ⁴³ L. A. Hadwiger, D. F. Kendra, B. W. Fristensky, W. Wagoner, R. A. A. Muzzarelli *et al.*, in “Chitin in Nature and Technology”, Springer, US, 1986, pp. 209–214
- ⁴⁴ M. Justi, M. P. de Freitas, J. M. Silla, C. A. Nunes and C. A. Silva, *J. Mol. Struct.*, **1237**, 130405 (2021), <https://doi.org/10.1016/j.molstruc.2021.130405>
- ⁴⁵ J. Zhang, A. J. Corkett, J. van Leusen, U. Englert and R. Dronskowski, *Crystals*, **12**, 1377 (2022), <https://doi.org/10.3390/cryst12101377>
- ⁴⁶ G. Martemucci, C. Costagliola, M. Mariano, L. D’andrea, P. Napolitano *et al.*, *Oxygen*, **2**, 48 (2022), <https://doi.org/10.3390/oxygen2020006>
- ⁴⁷ A. A. Starkov, *Ann. N.Y. Acad. Sci.*, **1147**, 37 (2008), <https://doi.org/10.1196/annals.1427.015>
- ⁴⁸ S. N. Kertmen, I. Gonul and M. Kose, *J. Mol. Struct.*, **1152**, 29 (2018), <https://doi.org/10.1016/j.molstruc.2017.09.067>
- ⁴⁹ N. Chaiwong, P. Leelapornpisid, K. Jantanasakulwong, P. Rachtanapun, P. Seesuriyachan *et al.*, *Polymers*, **12**, 1445 (2020), <https://doi.org/10.3390/polym12071445>
- ⁵⁰ X. Sun, J. Zhang, Y. Mi, Q. Miao, W. Tan *et al.*, *J. Ocean. Limnol.*, **40**, 284 (2022), <https://doi.org/10.1007/s00343-021-0352-2>
- ⁵¹ S. Baliyan, R. Mukherjee, A. Priyadarshini, A. Vibhuti, A. Gupta *et al.*, *Molecules*, **27**, 1326 (2022), <https://doi.org/10.3390/molecules27041326>
- ⁵² P. J. Jarnaa, E. Jonsson, S. Latini, S. Dhar, R. Larsson *et al.*, *Cancer Res.*, **59**, 5751 (1999)